Proceedings of the 21st ICSMGE, Vienna, Austria, 14 – 19 June 2026. Pistrol, Adam & Schweiger (eds.)
Published by: ÖGG, Austrian Society for Geomechanics, Salzburg, Austria, ISBN 978-3-9503898-4-5
https://doi.org/10.53243/ICSMGE2026-1621

Seismic Earth Pressure on Basement Walls Underlain by Bedrock: A Numerical Study

Yong-Gook Lee, Choonghyun Lee, Duhee Park, Dongyeon Lee
Department of Civil and Environmental Engineering, Hanyang University, Seoul, South Korea, dpark@hanyang.ac.kr

ABSTRACT: The dynamic increment of earth pressure is a critical parameter in the seismic design of underground basement structures. Conventional analytical and empirical approaches for rigid walls often overlook two key factors: the flexibility ratio (F), representing the stiffness ratio between the structure and surrounding soil, and the aspect ratio (L/H) of the basement. In this study, comprehensive dynamic numerical analyses were conducted on various basement configurations underlain by bedrock and different soil profiles. Results show that both F and L/H significantly affect seismic earth pressure. Stiff basements with high L/H values experience larger seismic pressure increments, while flexible basements with low L/H values show reduced pressures. A new empirical equation, developed through regression analysis, incorporates both F and L/H, improving prediction accuracy over existing methods. Residual analysis confirms its reliability and absence of bias across all cases, making it practical for engineering applications.

KEYWORDS: Underground basement structure, aspect ratio, flexibility ratio, racking ratio, seismic earth pressure.

1 INTRODUCTION

Historically, underground structures were considered less vulnerable to seismic damage. However, past failures during the San Fernando earthquake and the Kobe earthquake highlight the need for rigorous seismic vulnerability assessments. The seismic performance of buried structures is often evaluated using empirical and analytical correlations between the flexibility ratio (F) and the racking ratio (R). R denotes the ratio of peak structural racking deformation to the free-field racking response, while F represents the relative stiffness of the structure and surrounding soil.

Basements differ from tunnels because their top slabs are typically exposed, without overlying soil, and thus are not subjected to shear stress on the roof slab. It remains unclear whether tunnel-based F–R correlations apply to basements. Instead, seismic performance assessments for basements typically rely on seismic earth pressure calculations from the Mononobe–Okabe (M–O) method (Mononobe & Matsuo 1929; Okabe, 1924), which was originally developed for yielding walls in dry, cohesionless soil. Subsequent developments, such as the generalized formula of Kim et al. (2010) and the empirical Seed–Whitman (S–W) method (Seed & Whitman 1970), expanded applicability by incorporating soil cohesion, wall adhesion, and external loads.

Numerous analytical and numerical studies have sought to refine seismic earth pressure estimation. Veletsos and Younan (1994, 1997) provided solutions for rigid and flexible cantilever walls, demonstrating reductions in dynamic pressure with increased wall flexibility. Psarropoulos et al. (2005) validated these results numerically, though the no-gapping assumption produced unrealistic near-surface tension. Ostadan (2005) analyzed basements on rock or stiff soil, finding pressure distributions between the M–O and Wood (1973) solutions, but without considering L/H as the key parameter for basements. Veletsos et al. (1995) and Wood (1973) highlighted the influence of L/H but assumed rigid structural behavior, neglecting relative soil–structure flexibility effects. Later, Vrettos et al. (2016) incorporated soil inhomogeneity, reporting notable reductions in wall pressure.

Recent work has emphasized the role of kinematic and inertial interaction (Brandenberg et al. 2015; 2017) and the variability of pressure distributions observed in centrifuge and numerical studies (Al Atik & Sitar 2010; Mikola et al. 2016; Wagner & Sitar 2016]. These investigations show that both F and L/H strongly influence the dynamic earth pressure coefficient (ΔK_{ae}) and its distribution. Despite this, no established framework accounts for both parameters when evaluating basement seismic response.

To address this gap, the present study conducts dynamic numerical analyses across a range of basement geometries, soil profiles, and input motions. The findings are used to develop an empirical procedure for estimating seismic earth pressure on basement walls that explicitly incorporates both F and L/H.

2 VALIDATION OF NUMERICAL MODEL

2.1 *Centrifuge Experiment Overview*

A 1/36 scale centrifuge test by Wagner and Sitar (2016) was used to validate the numerical model. The experiment involved a stiff basement wall, 13.23 m in prototype depth, braced at three levels and founded on 6.76 m of medium-dense Nevada sand. Testing was conducted at 36g to evaluate seismic earth pressure development on deep basement walls.

Figure 1 shows the base acceleration history and response spectrum. The material properties of the structure and sand are given in Table 1 and 4. Additional experimental details are available in Wagner and Sitar (2016).

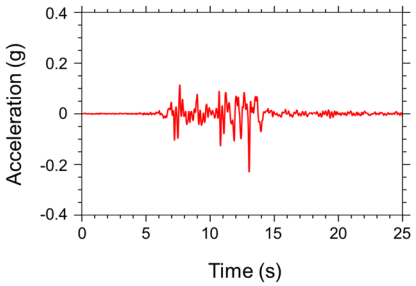

Figure 1. Achieved base ground motion time history

Table 1. Structure properties of model and prototype per unit width.

Basement	Property	Model	Prototype
Wall	Unit mass (kg/m^3)	2.8×10^{3}	2.8×10^{3}
	Cross section (m^2)	1.2×10^{-2}	5.8×10^{-1}
	Second moment of inertia (m^4)	4.5×10^{-7}	3.0×10^{-2}
Lateral bracing	Unit mass (kg/m^3)	3.3×10^{3}	3.3×10^{3}
	Cross section (m^2)	2.1×10^{-4}	9.5×10^{-3}
	Second moment of inertia (m^4)	1.5×10^{-8}	9.2×10^{-4}
Footing	Unit mass (kg/m^3)	2.7×10^{3}	2.7×10^{3}
	Cross section (m^2)	2.0×10^{-2}	9.1×10^{-1}
	Second moment of inertia (m^4)	1.1×10^{-6}	6.4×10^{-2}

Table 2. Properties of Nevada sand used in centrifuge test.

Specific gravity (G_s)	e_{min}	e_{max}	$\gamma_{d,min}$ (kN/m^3)	$\gamma_{d,max}$ (kN/m^3)
2.66	0.510	0.784	14.86	17.24

2.2 *Numerical Model Setup*

Dynamic simulations were performed using ABAQUS (SIMULIA, 2014). Four-node reduced-integration plane-strain elements (CPE4R) modeled the soil, while two-node beam elements (B21) represented the basement structure. The wall was modeled as linear elastic, and soil nonlinearity was incorporated via equivalent linear (EQL) properties.

Free-field boundary conditions were imposed through multi-point constraints (MPCs), replicating a simple shear condition along vertical boundaries. The soil–structure interface was modeled with a surface-to-node contact, applying a Coulomb friction coefficient defined as $\tan\varphi_{interface} = 2/3 \cdot \tan\varphi_{soil} \approx 0.33$ (Deng et al. 2016; Zhang et al. 2017). Normal behavior allowed separation without tensile stress transfer. Figure 2 illustrates the computational domain. The recorded base motion from the centrifuge test was applied at the model base to represent rigid boundary excitation.

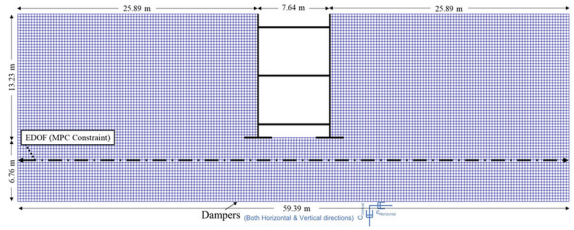

Figure 2. Two-dimensional numerical model.

2.3 *Soil Property Calibration*

The Nevada sand density profile was assumed to vary with depth following a normalized square-root distribution. The reference shear modulus from Hardin's correlation (Hardin, 1978). Small-strain shear modulus and shear wave velocity (V_S) profiles were derived from the mean effective confining pressure and atmospheric pressure.

Equivalent linear soil parameters were obtained from one-dimensional (1D) ground response analyses (GRA) in DEEPSOIL v.7 (DEEPSOIL, 2024) using the General Quadratic/Hyperbolic (GQ/H) model (Groholski et al. 2016). Nonlinear backbone curves were generated using Darendeli (2001), with OCR = 1.0, K$_0$ = 0.46, PI = 0, 10 loading cycles, and 1 Hz excitation. Rayleigh damping coefficients were assigned following Kwok et al. (2007), and damping curves were fit using the non-Masing rule (Phillips & Hashash 2009).

Effective shear strains for each layer were taken as 65% of the maximum strain from the GRA. These strains were used to compute the final EQL parameters assigned to the 2D ABAQUS model for dynamic simulations.

2.4 *Model–Experiment Comparison*

The numerical results at basement locations were evaluated against the centrifuge test data to verify model performance. Figure 3 compares the computed and measured free-field response spectra. Although some differences are observed, the numerical results show reasonably good agreement with the experimental records. A consistent shift toward longer periods was observed in the calculated spectra, likely due to two factors:

1. Soil profile approximation: The model used Hardin's (1978) correlation with a square-root density distribution following Wagner and Sitar (2016), which may not fully capture actual site conditions.
2. Equivalent linear simplification: The EQL approach, selected for its practicality in a generalized framework, reduces the complexity of nonlinear soil behavior under strong shaking, potentially influencing spectral response.

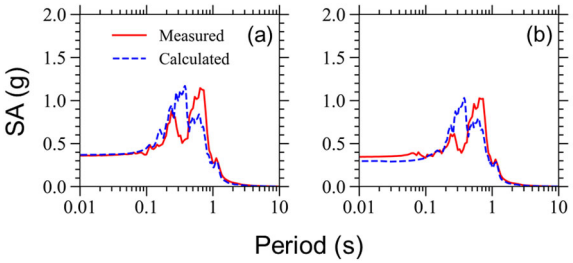

Figure 3. Comparison of measured and calculated free-field responses for response spectra at: (a) 2 m and (b) 4 m.

Figure 4 presents the computed ΔK_{ae} depth distributions, showing close alignment with centrifuge data. Overall, the use of EQL properties to approximate soil nonlinearity proved effective for capturing soil–basement interaction, and the adopted numerical procedure is considered robust for evaluating seismic earth pressures.

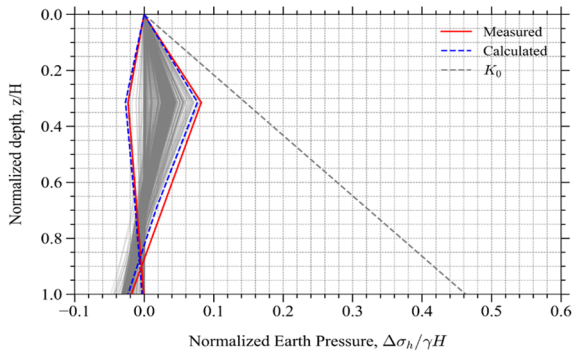

Figure 4. Comparison of normalized earth pressure along depth between measured and computed wall responses.

3 NUMERICAL MODELING FRAMEWORK FOR BASEMENT STRUCTURES

3.1 *Case Selection and Geometry*

Basement wall thickness was increased with depth to resist the higher lateral earth pressures at deeper levels. Multiple configurations with varying embedment depths and widths were analyzed to assess the influence of the L/H on seismic earth pressures. Two building heights were considered: three-story and five-story basements, each with a floor height of 4 m. The H ranged from 8 m to 16 m, and L from 8 m to 160 m, corresponding to L/H ratios of 0.67, 0.8, 1.33, 2, 4, and 8.

3.2 *Site Profiles and Soil Characterization*

Six site profiles were developed for basements with different embedment depths (Table 7, Figure 10). The time averaged V_S ($V_{S,soil}$) ranged from 150 to 300 m/s for the 12 m profiles and from 150 to 400 m/s for the 20 m profiles. The $V_{S,soil}$ was computed as:

$$V_{S,soil} = \frac{H}{\sum_{i=1}^{n} \frac{\Delta z_{i,i}}{V_{S,i}}} \quad (1)$$

where Δz_i and $V_{S,i}$ denote the thickness and V_S of the i^{th} layer, respectively. Bedrock was assumed directly beneath the basement base to eliminate rocking effects, representing shallow bedrock conditions typical of inland Korean sites.

Bedrock V_S was set at 760 m/s. 1D GRAs were performed for all profiles to determine equivalent linear soil properties, with motions applied to an assumed elastic half-space.

3.3 *Ground Motion Selection*

Seven recorded rock-outcrop motions were selected from the NGA-West2 database maintained by the Pacific Earthquake Engineering Research (PEER) Center. Because EQL analysis cannot fully reproduce nonlinear soil behavior under strong shaking, motions were restricted to peak ground accelerations (PGA) below 0.4 g, in line with the findings of Stewart et al. (2008), which showed that EQL and nonlinear analyses agree reasonably for stiff soils and PGA < 0.4 g in the 0.1–100 Hz range. The acceleration response spectra are shown in Figure 5. The selected PGAs range from 0.10 g to 0.36 g.

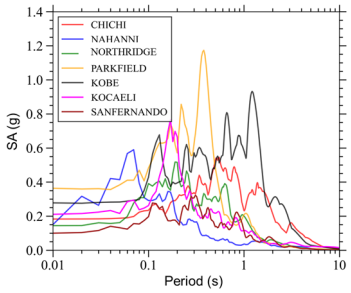

Figure 5. Response spectra of input motions.

4 DEVELOPMENT OF EMPIRICAL CORRELATION FOR DYNAMIC EARTH PRESSURE

4.1 *Evaluation of Simulated Seismic Earth Pressure*

Figure 6 and Figure 7 present the variation of ΔK_{ae} with both PGA_surface and PGA_averaged for L/H = 4. Following the approach in the preceding section, the data are grouped into stiff and flexible basement configurations. The results indicate that ΔK_{ae} is strongly influenced by F and generally increases with larger L/H ratios, emphasizing the need to consider both parameters in seismic earth pressure estimation.

When plotted against PGA_surface (Figure 6), the Seed and Whitman (1970) method slightly overestimates ΔK_{ae}. It substantially overpredicts values for L/H = 4. In comparison, the Mononobe–Matsuo (1929) method and Wood's (1973) elastic solution tend to produce even greater overestimations.

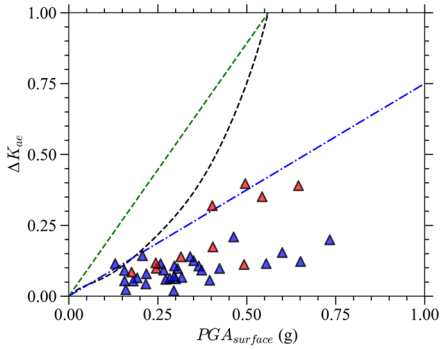

Figure 6. Comparison of ΔK_{ae} with $PGA_{surface}$ and analytical solutions for stiff, flexible three- and five-story basements with L/H = 4.

Against $PGA_{averaged}$ (Figure 7), the results exhibit reduced scatter, confirming that $PGA_{averaged}$ is a more consistent predictor of ΔK_{ae} than $PGA_{surface}$. For stiff basements with $PGA_{averaged}$ > 0.3g, the M–O method yields accurate predictions for L/H = 4. The S-W method underestimates ΔK_{ae} for L/H = 4. For flexible basements, it overestimates ΔK_{ae} and Wood's solution consistently overpredicts values for L/H = 4. These comparisons underscore that while the analytical methods are widely used, their assumptions of limit equilibrium for M–O and S–W, elastic theory for Wood—differ substantially from the EQL-based numerical approach adopted here, which iteratively accounts for soil stiffness and damping changes.

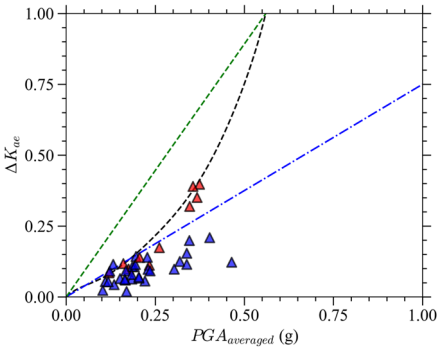

Figure 7. Comparison of ΔK_{ae} with $PGA_{averaged}$ and analytical solutions for stiff, flexible three- and five-story basements with L/H = 4.

4.2 *Proposed Empirical Correlation for* ΔK_{ae}

Given the limitations of existing equations, a new empirical model is developed to predict ΔK_{ae}, explicitly incorporating the effects of $PGA_{averaged}$, F, R, and L/H (Equation 2).

$$\frac{\Delta K_{ae}}{R \times PGA_{averagcd}} = \frac{lnR - 0.667}{0.05/F - 3.2} + \frac{L/H}{7.40R + 0.89L/H} \qquad (2)$$

Figure 8 compares the logarithmic residuals between measured ΔK_{ae} and predictions from the proposed and existing methods, binned by 0.2g increments of $PGA_{averaged}$. Wood's solution systematically overpredicts, while the M–O method generally overestimates. The S–W method often overpredicts yet yields plausible estimates for L/H = 4. The proposed equation produces significantly smaller residuals demonstrating improved predictive capability across the studied range.

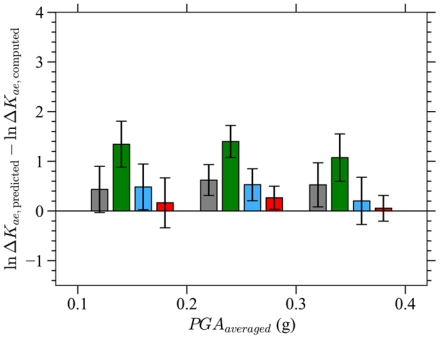

Figure 8. Residual comparison of ΔK_{ae} to $PGA_{averaged}$ bins with analytical solutions for stiff and flexible three-story basements with L/H =4.

5 CONCLUSIONS

Conventional approaches for estimating seismic earth pressure on basement walls typically adopt formulations developed for rigid retaining walls, neglecting the influence of F as well as L/H. This study aims to explicitly incorporate these two parameters into the prediction framework for seismic earth pressures on basements founded on bedrock. The analysis is limited to soil–basement interaction, excluding the superstructure's influence.

A series of EQL dynamic analyses were conducted to evaluate racking deformation and dynamic wall pressures, with the 2D numerical model validated against centrifuge test data.

The F, widely used in tunnel design but rarely in basement wall studies, was adopted to quantify soil–structure stiffness contrast.

The study evaluated the ΔK_{ae}. Results confirmed that both F and L/H significantly affect ΔK_{ae}: flexible basements exhibit notably lower ΔK_{ae} than stiff basements, and larger L/H values produce higher ΔK_{ae} due to reduced interaction forces and racking displacements. Using $PGA_{averaged}$ rather than $PGA_{surface}$ was found to reduce scatter in predictions.

6 ACKNOWLEDGEMENTS

This work was supported by the National Research Foundation of Korea (NRF) grant funded by the Korean Government (MSIT) (No. NRF-2022R1A2C3003245) and by the Basic Science Research Program through the NRF funded by the Ministry of Education (No. RS-2025-25438443).

7 REFERENCES

Al Atik, L., Sitar, N. (2010) Seismic earth pressures on cantilever retaining structures. J. Geotech. GeoEnviron. Eng. 136(10), 1324-1333. https://doi.org/10.1061/(ASCE)GT.1943-5606.0000351

Brandenberg, S.J., Mylonakis, G., Stewart, J.P. (2015) Kinematic framework for evaluating seismic earth pressures on retaining walls. J. Geotech. GeoEnviron. Eng. 141(7), 04015031. https://doi.org/10.1061/(ASCE)GT.1943-5606.0001312

Brandenberg, S.J., Mylonakis, G., Stewart, J.P. (2017) Approximate solution for seismic earth pressures on rigid walls retaining inhomogeneous elastic soil. Soil Dyn. Earth. Eng. 97, 468-477. https://doi.org/10.1016/j.soildyn.2017.03.028

Darendeli, M.B. (2001) Development of a new family of normalized modulus reduction and material damping curves. Ph.D. Dissertation. University of Texas at Austin

DEEPSOIL. (2024). A nonlinear and Equivalent Linear Seismic Site Response of 1-D Soil Columns, User Manual. V7.0. Board of Trustees of University of Illinois at Urbana-Champaign, Urbana, IL. University of Illinois at Urbana-Champaign

Deng, Y.H., Dashti, S., Hushmand, A., Davis, C., Hushmand, B. (2016) Seismic response of underground reservoir structures in sand: evaluation of class-c and c1 numerical simulations using centrifuge experiments. Soil Dyn. Earth. Eng. 85, 202-216. https://doi.org/10.1016/j.soildyn.2016.04.003

Groholski, D.R., Hashash, Y.M., Kim, B., Musgrove, M., Harmon, J., Stewart, J.P. (2016) Simplified model for small-strain nonlinearity and strength in 1D seismic site response analysis. J. Geotech. GeoEnviron. Eng. 142(9), 04016042. https://doi.org/10.1061/(ASCE)GT.1943-5606.0001496

Hardin, B.O. (1978) The nature of stress-strain behavior for soils. ASCE Geotechnical Engineering Division Specialty Conference, Pasadena, California; 1:3-90.

Hushmand, A., Dashti, S., Davis, C., Hushmand, B., McCartney, J.S., Hu, J., Lee, Y. (2016) Seismic performance of underground reservoir structures: insight from centrifuge modeling on the influence of backfill soil type and geometry. Journal of Geotechnical Geoenvironmental Engineering 142(11), 04016058. https://doi.org/10.1061/(ASCE)GT.1943-5606.0001544

Hushmand, A., Dashti, S., Davis, C., McCartney, J., Hushmand, B. (2016) A centrifuge study of the influence of site response, relative stiffness, and kinematic constraints on the seismic performance of buried reservoir structures. Soil Dyn. Earth. Eng. 88, 427-438. https://doi.org/10.1016/j.soildyn.2016.06.011

Kim, W.-C., Park, D., Kim, B. (2010) Development of a generalised formula for dynamic active earth pressure. Geotechnique 60(9), 723-727. https://doi.org/10.1680/geot.09.T.001

Kwok, A.O.L., Stewart, J.P., Hashash, Y.M.A., Matasovic, N., Pyke, R., Wang, Z., Yang, Z. (2007) Use of exact solutions of wave propagation problems to guide implementation of nonlinear seismic ground response analysis procedures. J. Geotech. GeoEnviron. Eng. 133(11), 1385-1398. https://doi.org/10.1061/(ASCE)1090-0241(2007)133:11(1385)

Mikola, R.G., Candia, G., Sitar, N. (2016) Seismic earth pressures on retaining structures and basement walls in cohesionless soils. Journal of Geotechnical Geoenvironmental Engineering 142(10), 04016047. https://doi.org/10.1061/(ASCE)GT.1943-5606.0001507

Mononobe, N., Matsuo, H. (1929) On the determination of earth pressures during earthquakes. World Engineering Congress, Tokyo, Japan; 9:177-185.

Okabe, S. (1924) General theory on earth pressure and seismic stability of retaining wall and dam. Journal of Japan Society of Civil Engineers 10(6), 1277-1323.

Ostadan, F. (2005) Seismic soil pressure for building walls: An updated approach. Soil Dyn. Earth. Eng. 25(7-10), 785-793. https://doi.org/10.1016/j.soildyn.2004.11.035

Penzien, J. (2000) Seismically induced racking of tunnel linings. earthquake Engineering and Engineering Vibration 29(5), 683-691.

Phillips, C., Hashash, Y.M. (2009) Damping formulation for nonlinear 1D site response analyses. Soil Dyn. Earth. Eng. 29(7), 1143-1158. https://doi.org/10.1016/j.soildyn.2009.01.004

Psarropoulos, P., Klonaris, G., Gazetas, G. (2005) Seismic earth pressures on rigid and flexible retaining walls. Soil Dyn. Earth. Eng. 25(7-10), 795-809.

Seed, H.B., Whitman, R.V. (1970) Design of Earth Retaining Structures for Dynamic Loads. ASCE Specialty Conference on Lateral Stresses in the Ground and Design of Earth Retaining Structures, Ithaca, New York; 103-147.

SIMULIA. (2014). ABAQUS Analysis User's Manual. 6.14. Dassault Systemes Simulia, Inc.

Stewart, J.P., Kwok, A.O.-L., Hashash, Y.M.A., Matasovic, N., Pyke, R., Wang, Z., Yang, Z. (2008) Benchmarking of nonlinear geotechnical ground response analysis procedures. Pacific earthquake engineering research center, University of California, Berkeley, 1-186.

Veletsos, A.S., Parikh, V., Younan, A.H. (1995) Dynamic response of a pair of walls retaining a viscoelastic solid. Earthquake Engineering and Structural Dynamics 24(12), 1567-1589. https://doi.org/10.1002/eqe.4290241203

Veletsos, A.S., Younan, A.H. (1994) Dynamic modeling and response of soil-wall systems. Journal of Geotechnical Engineering 120(12), 2155-2179. https://doi.org/10.1061/(ASCE)0733-9410(1994)120:12(2155)

Veletsos, A.S., Younan, A.H. (1997) Dynamic response of cantilever retaining walls. J. Geotech. GeoEnviron. Eng. 123(2), 161-172. https://doi.org/10.1061/(ASCE)1090-0241(1997)123:2(161)

Vrettos, C., Beskos, D.E., Triantafyllidis, T. (2016) Seismic pressures on rigid cantilever walls retaining elastic continuously non-homogeneous soil: an exact solution. Soil Dyn. Earth. Eng. 82, 142-153. https://doi.org/10.1016/j.soildyn.2015.12.006

Wagner, N., Sitar, N. (2016) On seismic response of stiff and flexible retaining structures. Soil Dyn. Earth. Eng. 91, 284-293. https://doi.org/10.1016/j.soildyn.2016.09.025

Wood, J.H. (1973) Earthquake-induced soil pressures on structures. Ph.D. Dissertation. California Institute of Technology

Zhang, W., Esmaeilzadeh Seylabi, E., Taciroglu, E. (2017) Validation of a three-dimensional constitutive model for nonlinear site response and soil-structure interaction analyses using centrifuge test data. International Journal for Numerical and Analytical Methods in Geomechanics 41(18), 1828-1847. https://doi.org/10.1002/nag.2702